Multi-objective Aerodynamic Optimization of High-speed Trains in Tunnels

J. Munoz-Paniagua, J. Garcia, A. Crespo

Abstract A genetic algorithm (GA) is employed for the multi-objective shape optimization of the nose of a high-speed train. Aerodynamic problems observed at high speeds become still more relevant when traveling along a tunnel. The objective is to minimize both the aerodynamic drag and the amplitude of the pressure gradient of the compression wave when a train enters a tunnel. The main drawback of GA is the large number of evaluations need in the optimization process. Metamodels-based optimization is considered to overcome such problem. As a result, an explicit relationship between pressure gradient and geometrical parameters is obtained.

1 Introduction

Importance of trains as a mean of transportation has notably grown in the last years because of its energy efficiency. This situation has attracted much attention from researchers to improve train aerodynamic performance. Efforts have been concentrated to the design of high-speed trains, exceeding over 300 $\mathrm{km\,h^{-1}}$, especially in densely populated areas of Western Europe, Japan or South Korea [1]. Such evolution has introduced aerodynamic problems that were neglected before, but are remarkably significant nowadays. Examples of these are aerodynamic drag, aerodynamic noise and vibration, or uprise of ballast. These problems become even more complicated and serious when train travels at high speed through a gallery like a tunnel.

Presence of tunnels is unavoidable in railways, and actually many reasons let us conclude that there will be even more (environmental considerations in densely populated areas or desire for straighter tracks for high-speed operation), [2]. Fur-

J. Munoz-Paniagua
Dpto. Ingeniería Energética y Fluidomecánica, Universidad Politécnica de Madrid, C/José Gutiérrez Abascal 2, 28006 Madrid, Spain, e-mail: le.munoz@upm.es

thermore, in the near future, most of the new tunnels are planned to be double-tube tunnels with only one rail per tube, driving to a reduction of the cross-sectional area at the tunnel (and consequently a larger blockage ratio); and it is hoped to even increase travel speed along the tunnel [3]. So, it is clear that aerodynamic optimization involving high-speed trains running through a tunnel is of major interest.

The aerodynamic consequences of high-speed trains running in a tunnel are basically resumed in two correlated phenomena, the generation of pressure waves and an increase in aerodynamic drag. Schetz [2] indicates that drag increase is more relevant in long tunnels, while pressure pulses generated at the extremes of the gallery cause the most problems in short length tunnels. Thus, high-speed train aerodynamic optimization becomes a multi-objective optimization problem. The present paper deals with the nose geometry optimization to reduce the pressure gradient of the compression wave when the train enters the tunnel.

2 Phenomena description and optimization approach

The flow generated by a train moving along a tunnel is characterized by strong unsteadiness because of the propagation and reflection of pressure waves. When a train enters a tunnel, a compression wave is generated, which propagates along the tunnel at approximately the speed of sound. Any discontinuity in the tunnel cross-section drives to a new reflection of the pressure wave. In particular, at the exit, part of the compression wave is reflected back as an expansion wave. The rest of it, namely micro-pressure wave, is reflected outside as an impulsive noise wave. The micro-pressure wave increases with the rate of change of the compression wave, *i.e.*, the pressure gradient ($\partial p/\partial t$), hence the effort to reduce the latter. The amplitude of the pressure gradient of compression wave is also responsible for the aural discomfort of train passengers.

The most relevant parameters affecting the pressure waves nature are blockage ratio, nose length, nose and tail shape, train speed and others related to the tunnel entrance design. Among them, a conscious description of the nose geometry of the train is accepted as the most relevant countermeasure in reducing $\partial p/\partial t$. The pressure gradient as a function of the nose shape is the objective function to minimize.

Raghunathan, [4], gives an expression of the peak pressure of the impulse wave as a function of the maximum pressure gradient in the compression wave front

$$\Delta p_{pulse,max} = \frac{A_t}{\pi r a_0} \left(\frac{\partial \Delta p}{\partial t} \right)_{comp,max} \tag{1}$$

being A_t the cross-section area of the tunnel, r a given distance away from the sound source, and a_0 the sound speed at atmospheric conditions.

Howe gives an expression for the maximum pressure gradient for a snub-nosed train entering an unflanged circular cylindrical tunnel of radius R along the axis of symmetry,

$$\left(\frac{\partial \Delta p}{\partial t}\right)_{comp,max} = \frac{\rho_0 v^3}{R}\frac{A}{A_t}\left(\frac{0.64+1.3M^6}{1-M^2}\right) \tag{2}$$

being A the train cross-sectional area and v the train speed. Nonetheless, this expression is independent of nose shape, whereas Matsuo, [5], proposes a formula to determine the peak pressure gradient as

$$\left(\frac{\partial \Delta p}{\partial t}\right)_{comp,max} = \frac{v}{\pi k d_t}\Delta p \tag{3}$$

with d_t the train hydraulic diameter and Δp the pressure rise due to the train entry in the tunnel. The coefficient k in equation 3 is a correction factor which considers the nose-geometry effect on pressure gradient. A modified equation of Ozawa approach is also included in [5] to determine Δp

$$\Delta p = \frac{1}{2}\gamma\rho M^2\left\{\frac{1-\phi^2}{\phi^2+(1-\phi^2)M-\gamma M^2(1-\frac{\phi^2}{2})}\right\} \tag{4}$$

where ϕ is defined as

$$\phi = 1-\frac{A}{A_t} \tag{5}$$

Previous studies indicate that the optimal nose shapes have much blunter front ends [6, 7]. This characteristic that is positive for reducing pressure gradient becomes a drawback when considering the drag coefficient. As drag coefficient causes up to 80% of total resistance when train speed is close to 300 $\mathrm{km\,h^{-1}}$, this is the other objective function to be optimized.

Optimization of aerodynamic properties of high-speed trains has been handled as a trial-and-error procedure, which relies on engineers experience. Multiobjective behaviour requires a compromise between the objective functions. Thus, a rigorous numerical algorithm that is capable of analyzing a design space. To deal with this problem, different optimization methods have been introduced and used int the aerodynamics research community. Two main groups are observed. Zero-order methods based on direct evaluations of the objective function, among which Genetic Algorithms (GA) stand out; and first-order methods based on gradient computation, where Adjoint methods are considered as the most efficient proposal. Advantages and disadvantages of each one have been pointed out. There is not a best one, and the choice of each one depends on the problem to be faced. Regarding the nature of the aerodynamics of train/tunnel systems, a three-dimensional, unsteady, turbulent, compressible flow is observed. Unsteadiness and compressibility implies an extra computational cost which needs to be limited in order to perform an efficient study. For this, Adjoint methods are postulated as the best option, as the number of numerical simulation required is inferior to the one involved in GA methods. However, the adjoint solver implemented in any commercial CFD code does not permit unsteady or compressible flow simulations yet, so the adjoint method option is discarded.

GA, introduced by Holland and developed by Goldberg [8], are a technique that mimic the mechanics of natural evolution. Once a population of potential solutions is defined, it combines survival-of-the-fittest concept to eliminate unfit characteristics and utilizes random information exchange, with exploitation of knowledge contained in old solutions, to effect a search mechanism with power and speed[2]. Iteratively, better results are obtained until a solution closer to globally optimal solution is reached. However, the main drawback when using GA is their need of a large number of evaluations of the objective function. Furthermore, this problem is considerably more important when evaluations are computational cost-effective. This number of simulations is defined by the number of design variables to represent any optimal candidate. Thus, the unsteady and compressible nature of the flow to be simulated make us to propose a very simple parameterization of the train nose. It is evident that the evaluation of each optimal candidate with the GA cannot be done by a solver call. Instead, a metamodel is considered as essential for the global search of the optimum. The metamodel technique chosen in this paper is the radial basis function (RBF) network, which is possible to be fitted and trained independently of the number of design variables used for the geometric parameterization. More information of it is indicated in section 7.

3 Description of the geometric parameterization

It has been explained that it is necessary to propose a geometric parameterization simple enough to make this optimization study affordable in terms of computational cost. The parameterization here presented is based on a baseline geometry. This reference geometry is called 'generic train', [9]. From it, one extra design variable is introduced here to give more diversity to the design space and capture the nose bluntness effect. Any optimal candidate is defined in terms of three design variables, l_1, l_2 and R_1. The nose length l_1 controls the shrinking of the nose and, following Raghunathan proposal [4], l_1 varies from one to four times the train width. The length l_2 refers to the bluntness of the nose (top view), and its range of variation is $[\frac{1}{6}w, \frac{1}{3}w]$, where w is the train width. Finally, radius R_1 defines the A-pillar roundness and let us change the cross-sectional area of the train and the bluntness of the nose tip. R_1 varies from $[\frac{1}{6}w, \frac{1}{4}w]$. This parameterization is sketched in figure 1. Geometries are parametrically defined in CATIA®. Height H and width w are set constant for all the geometries. H is 3.850 m and w is 3.000 m. Nose tip height and tip roundness are also the same for all the cases, with r_t = 0.750 m. Clearance c between the top of the rail and the bottom of the train is set to 0.250 m. The radius that controls the connection between the nose and the rest of the car is $r_c = 0.750$ m.

A three-dimensional 'maximin' Latin Hypercube design (LHD) of fifteen points (size = $5n$, where n is the dimensionality of the design space) is used to generate the DoE. A database of the best designs of LHD is included in [10], from where the design used here is obtained. In table 3 information of the fifteen geometries that

define the initial DoE is presented. Values of the three design variables are given, and geometrical characteristics to compare them are also included. The cross-sectional area of the train and the corresponding blockage ratio is computed. A cross-sectional area of the tunnel of $A_t = 63$ m^2 is considered. It is observed that as the radius R_1 becomes larger, the train frontal area reduces. This effect might lead to a mistaken conclusion when comparing the aerodynamic drag among the proposed geometries, since it is obvious that a smaller cross-sectional area produces a lower pressure drag. However, range of variation of R_1, is limited so that cross-sectional area changes are negligible, which is emphasized regarding the blockage ratio. R varies between 0.176 and 0.180, what is assumed to be acceptable for further comparisons.

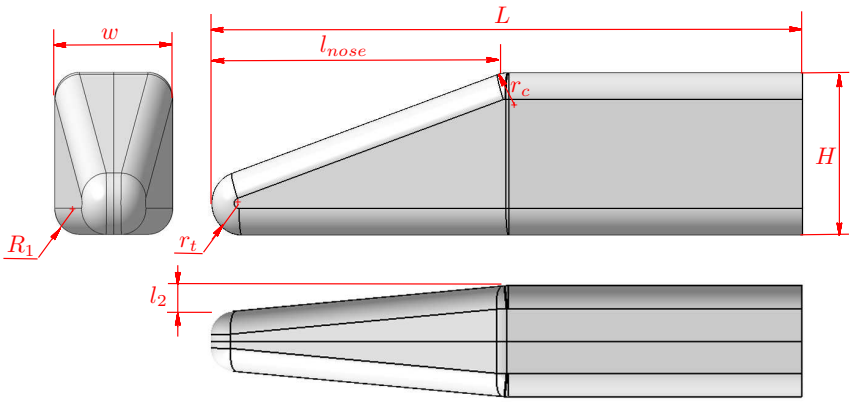

Fig. 1 Geometric parameterization used to define the optimal candidates.

4 Numerical set-up

The computational domain is composed of the tunnel and the tunnel entrance. As the purpose of this study is to analyze the unsteady flow field at the tunnel entrance to determine the pressure gradient when the train enters the tunnel, outside region of the tunnel end is not included in the computation. This situation is also known as infinite length tunnel. The train width is taken as the reference length. The tunnel is 100.0 (300.0 m) long, which is long enough to permit an investigation of the transient flow field at the tunnel entry, [5]. The railway is simple-tracked, so the train body is placed at the center of the tunnel section. Figure **??** presents a front view of the train and the tunnel. The train is 1.285 high and the clearance is 0.083 high.

Geo #	l_1 [m]	l_2 [m]	R_1 [m]	A [m^2]	R
1	3.000	0.679	0.607	11.195	0.178
2	3.643	0.929	0.571	11.270	0.179
3	4.286	0.643	0.732	11.090	0.176
4	4.929	0.893	0.696	11.134	0.177
5	5.571	0.536	0.536	11.304	0.179
6	6.214	0.786	0.500	11.335	0.180
7	6.857	0.500	0.661	11.175	0.177
8	7.500	0.750	0.625	11.215	0.178
9	8.143	1.000	0.589	11.252	0.179
10	8.786	0.714	0.750	11.067	0.176
11	9.429	0.964	0.714	11.112	0.176
12	10.071	0.607	0.554	11.287	0.179
13	10.714	0.857	0.518	11.320	0.180
14	11.357	0.571	0.678	11.155	0.177
15	12.000	0.821	0.643	11.195	0.178

Table 1 Design variable values and geometrical characteristics of the geometries included in the initial design of space. A refers to the train cross-sectional area, while R is the blockage ratio.

At the beginning of the computation, the train should ideally be far from the tunnel. Although this requires a great deal of computational time cost, as schematically illustrated in figure 2, here an intermediate zone of 50.0 (150 m) long is considered upstream the train nose before entering the tunnel. This is used to stabilize the numerical simulation. In order to not consider the effect of the tail entering the tunnel, an infinite length train is modeled. Actual length of the train model is 67.0 (200 m). The surroundings of the entrance of the tunnel are dimensioned so that the domain boundaries do not affect the flow close to the tunnel portal. The boundaries are 10.0 (30.0 m) far from the longitudinal symmetry axis of the train

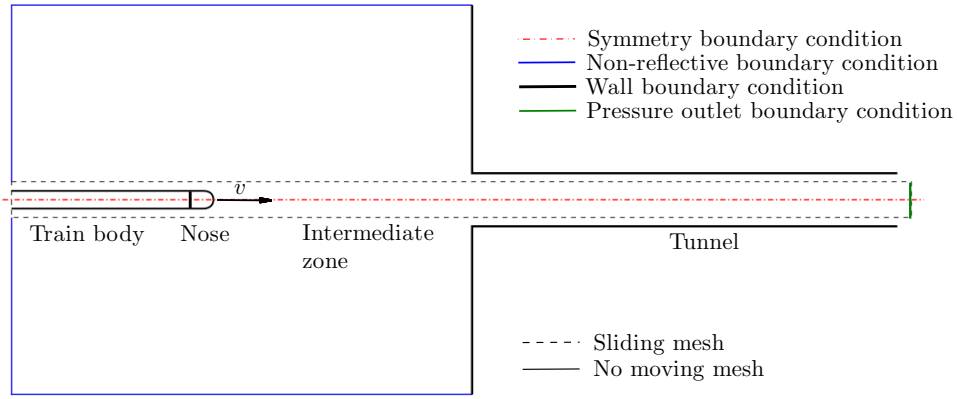

Fig. 2 Dimensions of the flow domain and boundary conditions for the numerical simulations.

Simulations are run using ANSYS-FLUENT® CFD software. A compressible, unsteady, turbulent flow simulation is considered. The standard $k-\varepsilon$ turbulence model is used, with second order upwind momentum and time discretization scheme. A train speed of $v = 250$ km h^{-1} is imposed. The simulation of a train moving in a gallery involves the relative motion of the train with respect to the tunnel walls. This motion is modeled using the sliding mesh technique. Since the flow is inherently unsteady, a time-dependent approach is required. A time step has to be defined for that discrete steps. Here the time step Δt is 0.001. This time step is sufficiently small to resolve unsteadiness in the flow field. The boundary layer is captured all along the train surface and the ground, but not in the tunnel walls. Wall functions are used, and y^+ is fixed to 100. Boundary conditions are indicated in figure 2.

5 Validation of the numerical results

In [**?**] and [**?**] a relation of the pressure rise Δp and train velocity for different blockage ratios $R = \frac{A}{A_t}$ is given, with A the train cross-sectional area and A_t the cross-sectional area of the tunnel. Experimental data for $R = 0.216$ at real tunnels is included. These data are represented in figure 3, where the red dots refer to the experimental data. This information is used to validate our numerical results. While the numerical set up was validated from experimental data, the pressure rise values obtained from the numerical simulations of the geometries of the initial DoE are considered satisfactory as they are well agreed with the theoretical expression from equation 4. In figure 3, blue dots refer to the pressure rise observed in our cases.

6 Discussion of the initial geometries performance and flow field description

An analysis of the performance, in terms of pressure rise, maximum pressure gradient and drag coefficient, of the first fifteen geometries is developed before running the actual optimization process. It is considered interesting to do it in order to yield some insight into the nature of the design space.

Figure 4 shows the distribution of cross-sectional area of the train for the most representative cases included in the initial design of experiments. To complete it, distributions of an ellipsoid, a paraboloid and a conic nose are also plotted. The paraboloid of revolution is considered as the optimal geometry, as it involves a constant rate of change of cross-sectional area. However, Iida [6] proposes an optimal nose shape which has a blunter front end and a slower increase of the cross-sectional area in the middle section of the nose. All the geometries considered in this study have a blunter front end that the paraboloid, and geometries #1 and #3 are still

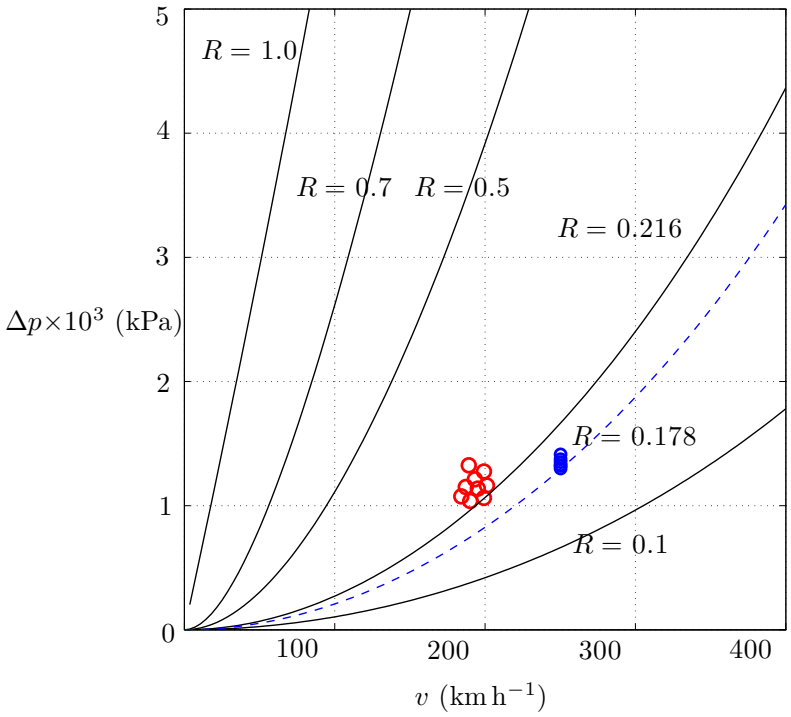

Fig. 3 Validation of the numerical results. It is represented in blue dots the pressure rise from the numerical simulations.

blunter than Iida proposal. A zoom of the rate of change at the front end is used to stress these differences.

Design variable l_1, which directly affects the shrinking or slenderness ratio of the nose, has little impact on the rate of change. Instead, l_2 and R_1 have an important effect on the bluntness of the nose. This behaviour is stressed when comparing the maximum pressure gradient for geometries of different nose lengths.

In figure 6, it is shown that the different design variables defining the nose shape have little influence on the maximum pressure level. Differences in the cross-sectional area of the train are evidenced in the different pressure rises, but these differences are negligible as it was expected from the blockage ratio values. However, the pressure evolution in time and the maximum pressure gradient are significantly dependent on the nose shape. Among the fifteen cases simulated, the geometry #1 is found to be the best in terms of the intensity of maximum pressure gradient. This conclusion is agreed with the observations of Maeda [**?**] or Kwon [11].

A reduction of the train nose accelerates the compression of the air. Consequently, an abrupt pressure rise is observed as it is shown in figure 6.

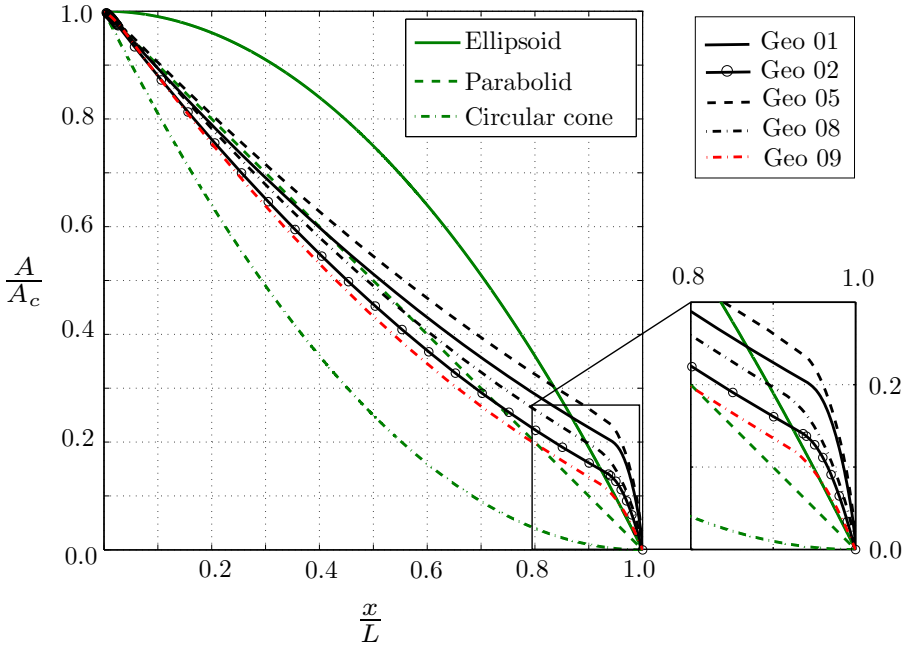

Fig. 4 Cross-sectional area distribution of the most representative geometries included in the initial DoE.

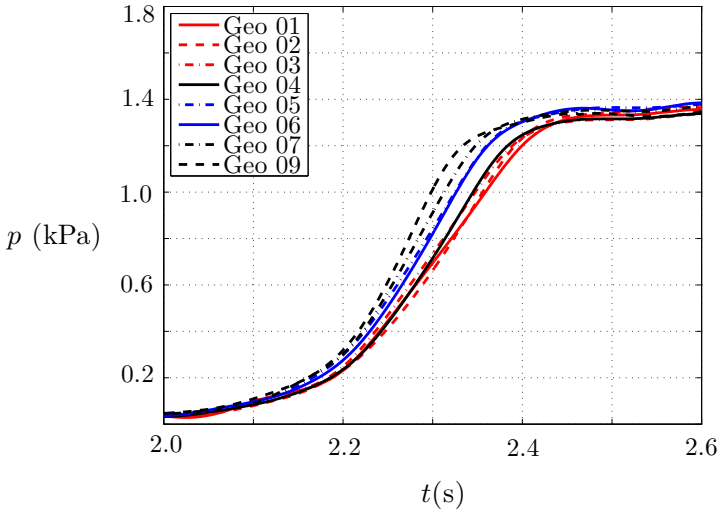

Fig. 5 Pressure rise at 75 m from the tunnel entrance result of the compression wave when the train enters the tunnel for the most representative geometries included in the initial DoE.

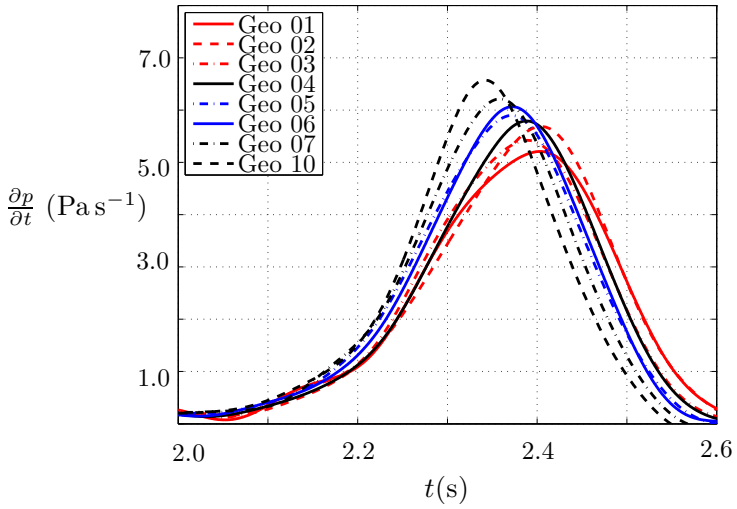

Fig. 6 Pressure gradient at 75 m from the tunnel entrance result of the compression wave when the train enters the tunnel for the most representative geometries included in the initial DoE.

7 Metamodel construction

Let consider a set of N data points $(\mathbf{x}_i,\ y_i)$, $i = 1 \ldots N$, where $\mathbf{x}_i$ denotes an $n-$dimensional vector of independent variables, $(x_i^1,\ x_i^2,\ \ldots x_i^n)$, and y_i is the value of the function at that point. Radial basis function (RBF) method is an interpolation technique based on the idea that every known point i 'influences' its surroundings the same way in all directions according to some assumed functional form $\phi(d_i)$, such that the radial distance d_i is defined as $d_i = |\mathbf{x} - \mathbf{x}_i|$ from (*i.e.* centered at) the point $\mathbf{x}_i$. The norm $||$ is the Euclidean distance. $\phi(d_i)$ is called the radial basis function, and RBF method uses a linear combination of m radial basis functions

$$\hat{y}(\mathbf{x}) = \sum_{i=1}^{m} \omega_i \phi(|\mathbf{x} - \mathbf{x}_i|) \tag{6}$$

to approximate the response $y(\mathbf{x})$. w_i is the weight of radial basis function i in the linear combination aforementioned. While equation 6 is linear in terms of the weights ω_i, the predictor $\hat{y}$ can approximate highly non-linear responses. A typical radial function is the Gaussian function

$$\phi(d_i) = \exp\left(-\frac{d_i^2}{2r_i^2}\right) = \exp\left(-\frac{|\mathbf{x} - \mathbf{x}_i|^2}{2r_i^2}\right) \tag{7}$$

An unavoidable task when using RBF networks is the estimation of the different parameters involved in its construction. Apart from setting the weights in equation 6,

the number of hidden units m, the spread r and the centers $\mathbf{x}_i$ are the other parameters to be defined.

The choice of centers affects the complexity and performance of the metamodel. If too few centers were used, the network may not be capable of generating a good approximation to the target function. If all the input samples are used as a set of centers of the network, the model may overfit the data and it may fit misleading variations due to imprecise or noisy data. To avoid it, forward selection is commonly used, [12]. The idea is to add new basis functions (or centers) until some chosen criterion, such as GCV (generalized cross-validation) stops decreasing. In this study, such strategy is not contemplated since the number of points in the DoE is not so large as to outline a notable benefit to select a subset of centers from the larger set of all the input samples. The number of neurons m is set equal to N, and the centers do coincide with the sampling points $\mathbf{x}_i$. The spread is fixed for all basis functions, and the value is first estimated by the relation $r = d_{max}/\sqrt{m}$, where d_{max} is the maximum distance between any two centers. This rule of dumb is just considered as the beginning of a parametric study of its effect on the performance of the network, see figure 8(a).

Instead of forward selection, ridge regression is used to control the model sensitivity. Ridge regression [12] is used to reduce the effective number of parameters, and the resulting loss of flexibility makes the model less sensitive, controlling the balance between bias and variance. A regularization parameter λ is introduced to the sum-squared-error expression applied to determine the optimal weight vector $\{\omega\}_{j=1}^{m}$. In [12], a parametric study to find the parameter λ is proposed, and this strategy is also used in this paper. The model selection criteria used to find λ (and r) are the prediction error sum of squares (PRESS)and the GCV, whose expressions are given as

$$PRESS = \hat{\sigma}^2_{LOO} = \frac{\mathbf{y}^T\mathbf{P}(\mathrm{diag}(\mathbf{P}))^{-2}\mathbf{P}\mathbf{y}}{N} \tag{8}$$

based on the leave-one-out cross-validation method. $\mathbf{P}$ is called the projection matrix, and $\mathbf{y}$ is the observation vector from the DoE. For a better understanding of each variable, the reader is referred to Orr [12]. Generalized cross-validation (GCV) is defined as

$$\hat{\sigma}^2_{GCV} = \frac{p\mathbf{y}^T\mathbf{P}^2\mathbf{y}}{(\mathrm{trace}(\mathbf{P}))^2} \tag{9}$$

In figures 8(a) and 8(b) it is shown the conclusions about the optimal value of λ and r. While the spread is increased, the prediction error is reduced, but the coefficient R^2 is lower than in the cases of smaller spread values. As the accuracy of the model measured by R^2 is still acceptable for the largest spread (r = 1.83), the criteria of best prediction (minimal σ_{LOO} or σ_{GCV}) is adopted as the model selection criteria. In such situation, lowest prediction error is observed for a λ = 0.01, which is considered as the regularization parameter. These coefficients do complete the metamodel definition before using it for the surrogate-based optimization process.

8 Surrogate-based optimization

Once the metamodel has been constructed, it is possible to carry out the actual optimization process. Here the MATLAB code implementation, included in the Optimization Toolbox, is used for running the genetic algorithm. According to the theory previously introduced, some operation parameters have to be fixed. Selection, crossover and mutation operators, respective crossover and mutation probabilities and population size are parameters that can strongly affect on the GA efficiency. Therefore, a parametric study to determine which values allow a best performance is necessary. Ten different population sizes (from 20 to 200 individuals per population) are tested. Crossover probability is also studied, varying it from P_c = 0.25 up to 1. Mutation probability is fixed to 0.01. Table 5 summarizes the most important information from the algorithm applied.

Population size	20 - 200
Elitism	Yes
# elite individuals	2
Selection function	Tournament (4)
Scaling function	Ranking
Crossover function	Two-points
P_c	0.25 - 1
Mutation function	Uniform
P_m	0.01
# max generations	300

Table 2 GA parameters values.

In this way, 160 tests are performed. The best combination of these parameters is selected regarding at the optimal found by the algorithm. It is obtained when P_c = 0.45 and the population size is 160. The optimal design results in the following design variables values. After generation fifteen, no improvement is observed in the best optimal candidate. The final result of the optimization process is a maximum pressure gradient of 5201 Pa s^{-1}.

Geo #	l_1 [m]	l_2 [m]	R_1 [m]
1	3.400	0.550	0.685

Table 3 Design variables of the optimal geometry resulting from the optimization process.

9 Conclusions

This paper shows the capabilities of Genetic Algorithms (GA) to solve an optimization problem when the entry of a high-speed train in a tunnel is considered. The nature of the flow, with a compressible, unsteady and turbulent behavior makes necessary to limit the number of design variables in order to run an efficient op-

timization resolution. In this paper a simple geometric parameterization based on three design variables have been proposed.

The high computational cost of a simulation makes as well necessary to base the optimization resolution on metamodels or surrogate models. Here a radial basis function (RBF) network has been considered to substitute the expensive accurate simulations by the evaluation of a very cheap model that helps speeding up the optimization process. This metamodel introduces new parameters that need to be set. The interest of using metamodels is based not only on accelearting the optimization process, but also on yielding insight the nature or landscape of the design space.

The limititations because of the cost of an unsteady compressible flow simulation result into a poor initial design of experiments, which directly affects the metamodel. Even when the accuracy and prediction characteristics of the metamodel are satisfactory, new simulations are required to enhance the model response.

This work is financed by Ministerio de Ciencia e Investigación (Eng. Ministry of Science and Technology) under contract TRA-2010-20582, included in the VI Plan Nacional de I+D+i 2008-2011. It is also part of the research project included in Subprograma INNPACTO, from Ministerio de Ciencia e Innovación.

References

1. P. Ricco and A. Baron and P. Molteni, Nature of pressure waves induced by a high-speed train travelling through a tunnel, *Journal of Wind Engineering and Industrial Aerodynamics*,**95**, 781–808 (2007)
2. J. A. Schetz, Aerodynamics of High-Speed Trains, *Annual Review of Fluid Mechanics*, **33**, 371–414 (2001)
3. D. Heine and K. Ehrenfried, Experimental study of the compression-wave generation due to train-tunnel entry, In proceedings of the *First International Conference on Railway Technology: Research, Development and Maintenance*, (2012)
4. R. S. Raghunathan, H.-D. Kim and T. Setoguchi, Aerodynamics of High-Speed Railway Train, *Progress in Aerospace Sciences*, **38**, 469–514 (2002)
5. M. Bellenoue, V. Moriniére and T. Kageyama, Experimental 3-D simulation of the compression wave, due to train-tunnel entry, *Journal of Fluids and Structures*, **16(5)**, 581–595 (2002)
6. T. S. Yoon, S. Lee, J. H. Hwang and D. H. Lee, Prediction and validation on the sonic boom by a high-speed train entering a tunnel, *Journal of Sound and Vibration*, **247(2)**, 195–211 (2001)
7. Yo-Cheon Ku and Joo-Hyun Rho and Su-Hwan Yun and Min-Ho Kwak and Kyu-Hong Kim and Hyeok-Bin Kwon and Dong-Ho Lee, Optimal cross-sectional area distribution of a high-speed train nose to minimize the tunnel micro-pressure wave, *Struct. Multid. Optim.*, **42**, 965–976 (2010)
8. D. E. Goldberg, Genetic Algorithms in Search, Optimization and Machine Learning, *Addison Wesley* (1989)
9. M. Sima, E. Grappein, M. Weise, N. Paradot, M. Hieke, C. Baker, R. Licciardello, M. Couturier, Presentation of the EU FP7 AeroTRAIN project and first results, In proceedings of the *9th World Congress on Railway Research*, Lille, France, May 22-26 (2011)
10. B. Husslage and G. Rennen and E. van Dam and D. den Hertog, Space-Filling Latin Hypercube Designs for Computer Experiments Social Science Research Network, (2008)
11. H.-B. Kwon, K.-H. Jang, Y.-S. Kim, K.-Y. Yee and D.-H. Lee, Nose Shape Optimization of High-Speed Train for Minimization of Tunnel Sonic Boom, *JSME International Journal Series C*, **44**, 890–899 (2001)
12. M. Orr, Introduction to Radial Basis Function Networks, April 1996

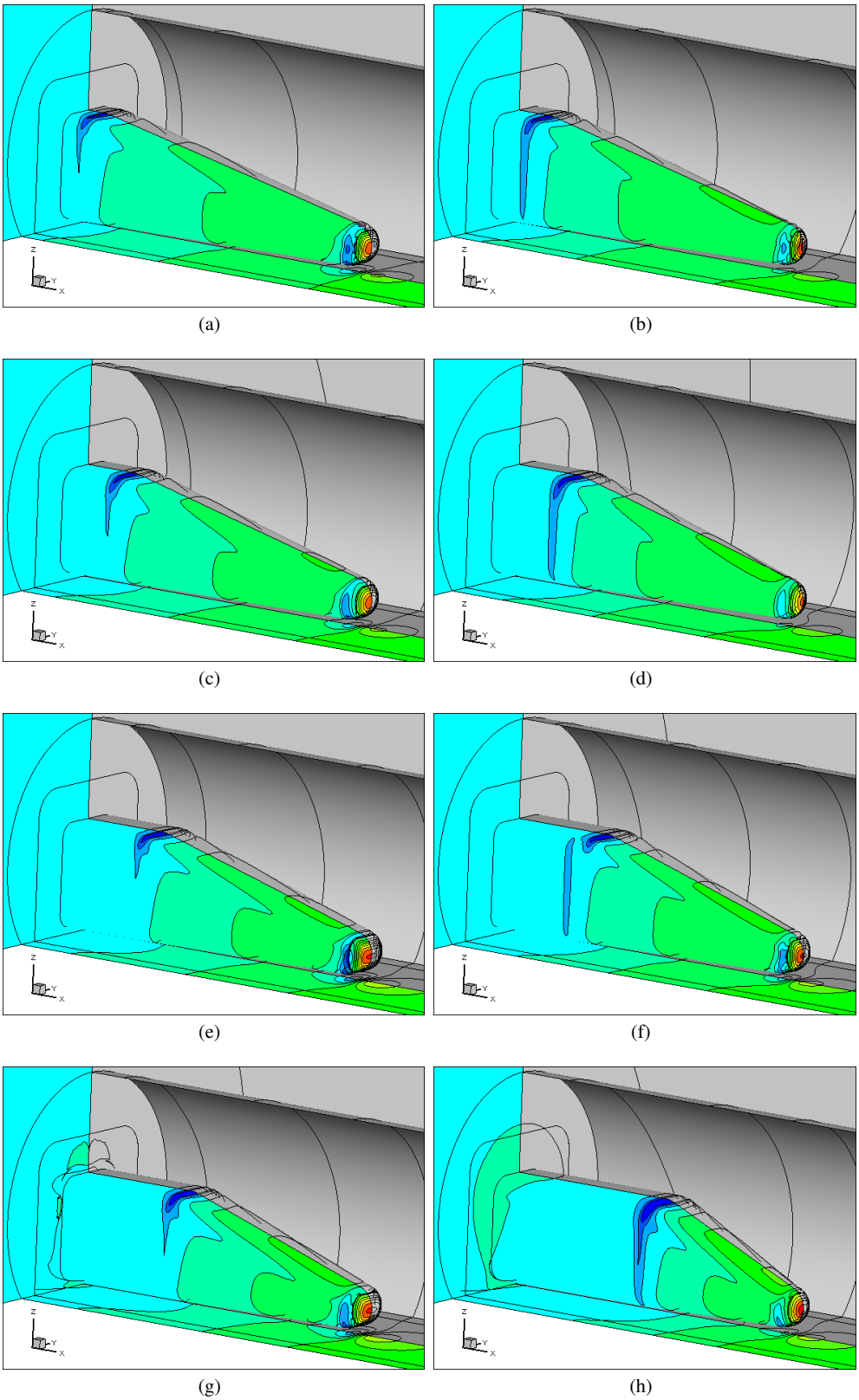

Fig. 7 Pressure fields at the train surface for the most characteristic trains. Geometries #1 (a), #2 (b),#3(c),#4(d),#5(e),#6(f),#7(g),#10 (h)

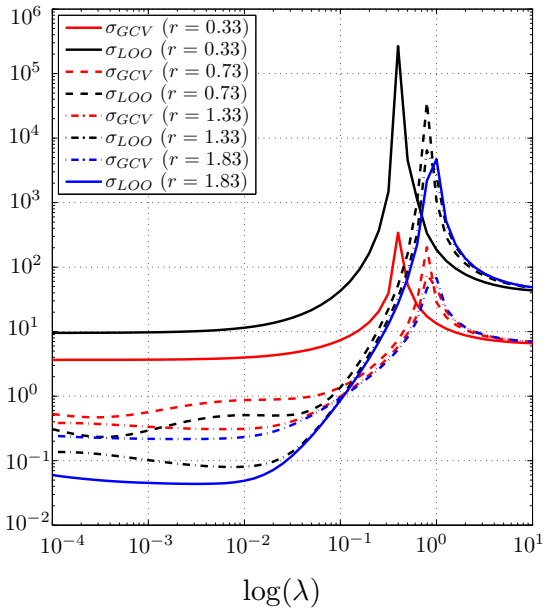

(a)

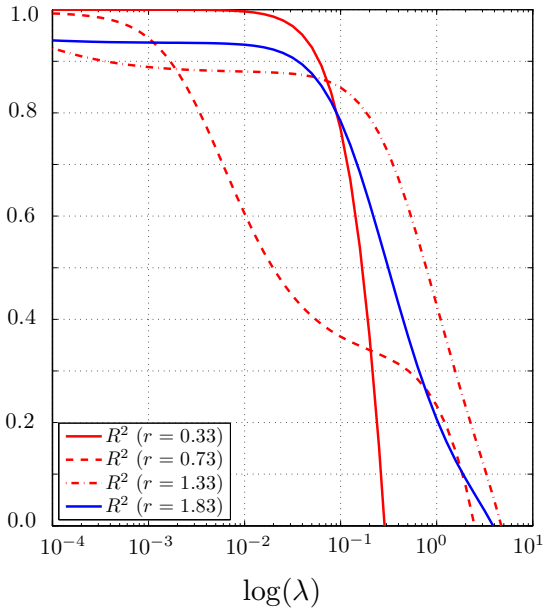

(b)

Fig. 8 Examples of three-dimensional shape parameterization and nose construction. Train bodies are constructed with CATIA®. Figure **(a)** corresponds to ICE 2.